https://doi.org/10.5194/egusphere-2024-1025
Preprint. Discussion started: 18 April 2024

A first attempt to model global hydrology at hyper-resolution

Barry van Jaarsveld[1], Niko Wanders[1], Edwin H. Sutanudjaja[1], Jannis Hoch[1,2], Bram Droppers[1], Joren Janzing[3,4,5], Rens L.P.H. van Beek[1], and Marc F.P. Bierkens[1,6]

[1]Utrecht University, Department of Physical Geography, Princeton laan 8a, Utrecht, The Netherlands
[2]Fathom, Bristol, United Kingdom
[3]Institute for Snow and Avalanche Research SLF, Davos Dorf, Switzerland
[4]Institute for Atmospheric and Climate Science, ETH Zurich, Zurich, Switzerland
[5]Climate Change, Extremes and Natural Hazards in Alpine Regions Research Center CERC, Davos Dorf, Switzerland
[6]Deltares, Unit DSubsurface and Groundwater Systems, Utrecht, The Netherlands

Correspondence: Barry van Jaarsveld (a.s.vanjaarsveld@uu.nl)

Abstract. Global hydrological models are one of the key tools that can help meet the needs of stakeholders and policy makers when water management strategies and policies are developed. The primary objective of this paper is therefore to establish a first of its kind, truly global hyper-resolution hydrological model that spans a multiple-decade period (1985 - 2019). To achieve this, two key limitations are addressed, namely the lack of high resolution meteorological data and insufficient representation of lateral movement of snow and ice. Thus a novel meteorological downscaling procedure that better incorporates fine-scale topographic climate drivers is incorporated, and a snow module capable of lateral movement of frozen water resembling glaciers, avalanches and wind movement is included. We compare this global 30 arc-seconds version of PCR-GLOBWB to previously published 5 arc-minutes and 30 arc-minutes versions by evaluating simulated river discharge, snow cover, soil moisture, land surface evaporation, and total water storage against observations. We show that hyper-resolution provides a more accurate simulation of river discharge, this is especially true for smaller catchments. We highlight that although global hyper-resolution modelling is possible with current computational resources and that hyper-resolution modelling results in more realistic representations of the hydrological cycle; our results suggest that global hydrological modelling still needs to incorporate landcover heterogeneity at the sub-grid scale and include processes relevant at the kilometre scale in search of better predictive capacity to provide more accurate estimates of soil moisture and evaporation fluxes.

1 Introduction

Water is a vital and cross-cutting element needed to achieve a number of sustainable development goals (Vörösmarty et al., 2015; Alcamo, 2019). Accurately simulating, predicting and forecasting the distribution, abundance, and shortage of water is therefore a crucial challenge for the hydrological community. By providing information on water resources, global hydrological models are one of the key tools that can help meet the needs of stakeholders and policy makers when water management strategies and policies are developed (Bierkens, 2015; Bierkens et al., 2015; Wood et al., 2011). Despite their usefulness, an ongoing critique against their use is that the resolution of these models are unable to provide relevant information at scales at which adaptation strategies are implemented by stakeholders (Wada et al., 2017). In response to this criticism, there has

https://doi.org/10.5194/egusphere-2024-1025
Preprint. Discussion started: 18 April 2024

been an effort to increase the spatial resolution of current state-of-the-art global hydrological models (Hoch et al., 2023). The drive to develop such hyper-resolution models is based on the assumption that increased resolution will provide stakeholders and policy makers with information on scales that are more relevant and actionable; which will in turn increase these model's impact and promote their application (Bierkens et al., 2015; Wood et al., 2011). Hyper-resolution global hydrological models are expected to better capture the relevant physical processes that shape the distribution and quantity of global water resources and their pursuit is also motivated by the benefits they may offer the broader scientific community; it has previously been described as one of hydrology's "grand challenges" (Bierkens et al., 2015).

To date, there has been noticeable progress towards a truly global hyper-resolution hydrological model; however, given the complexity of such an undertaking and the associated computational burden, hyper-resolution models have been confined to continental scale applications (e.g, Beven et al., 2015; Hoch et al., 2023; O'Neill et al., 2021; Vergopolan et al., 2021; Chaney et al., 2021). For example, the ParFlow model has been used to simulate groundwater and surface water for the contiguous United States at a spatial resolution of approximately 1 km (Yang et al., 2023). Also, for the contiguous United States, Aerts et al. (2022) analyzed how increasing the resolution from 3 km to 200 m in wflow_sbm affects predictions of river discharge. There has been an attempt to model the European continent at the 1km resolution; where Hoch et al. (2023) presents a 1 km version of PCR-GLOBWB over a multi-decade period. These studies have provided much needed headway towards truly global hyper-resolution modelling; but they have also brought to the fore a number of challenges that need to be overcome.

Challenges surrounding global hyper-resolution models are related to epistemic uncertainties in input data and whether models at these finer resolutions can effectively capture and reproduce processes that govern water dynamics (Hoch et al., 2023; Aerts et al., 2022; Yang et al., 2023). Previous studies on continental scale hyper-resolution models have raised the question whether an increased resolution results in a more accurate representation of the water cycle; there is mixed support for this notion. For example, when modelling at spatial resolutions approaching 1 km and comparing their accuracy to more coarse-scale counterparts, river discharge is more accurately simulated in some locations, while other locations show a reduced accuracy (Hoch et al., 2023; Aerts et al., 2022). Furthermore, there are discrepancies between how different components of the water cycle respond to an increase in model resolution. Hoch et al. (2023) experienced that, as resolution increases, the fidelity of soil moisture and total evaporation as simulated with the global hydrological model decreases, even though river discharge shows an increase in accuracy when moving to finer resolutions (Hoch et al., 2023). However, valuable the identification of such an inconsistency may be, perhaps more importantly, it provides for an opportunity to further understand how and why the different components of the water cycle respond to an increase in model resolution. Increases in model resolution have also highlighted the need for the inclusion of fine-scale processes that are be neglected at coarser resolutions. For example, Hoch et al. (2023) reports that in the absence of processes that represent the transport of frozen water through glaciers, avalanches and wind unrealistic accumulations of frozen water accumulate into snow towers. Despite these challenges, continental scale hydrological models have showed that it is possible to accurately simulate at least some components of the hydrological cycle at resolutions approaching ≈1 km (Hoch et al., 2023; Yang et al., 2023), albeit not yet at the global scale.

One source of uncertainty is the mismatch between model resolution and that of meteorological data used as forcing (Hoch et al., 2023). The lack of meteorological data at the appropriate resolution is a major limitation for both coarse- and fine-scale

https://doi.org/10.5194/egusphere-2024-1025
Preprint. Discussion started: 18 April 2024

models (Wilby et al., 2000; Benedict et al., 2019; Hoch et al., 2023; Yang et al., 2023; Döll et al., 2016; Müller Schmied et al., 2014). Available reanalysis products are created at a much coarser resolution than global hydrological models and fail to represent sub-grid climate dynamics that are important in defining local hydrological patterns. As a result, downscaling climate forcing becomes necessary for global hyper-resolution hydrological models and their accuracy is heavily dependent on how such downscaled products reflect reality. To date the production of global climate models at resolutions discussed here are constrained by technical limitations around storing the large volumes of output data storage and computational resources required to complete such simulations (Schär et al., 2020; Karger et al., 2017). However, recently 1 km meteorological data have become available in the form of climatologies as in the case of WordClim (Fick and Hijmans, 2017) and CHELSA (Karger et al., 2017; Brun et al., 2022), which could feasibly be used to downscale coarse daily meteorological forcing data from reanalyses to the required hyper-resolution.

Given these considerations, there is a need to assess the feasibility of a truly global hyper-resolution hydrological model that relies on improved spatial representation of meteorological data. The primary objective of this paper is therefore to establish a first of its kind, truly global hyper-resolution hydrological model that spans a multiple-decade period (1985 – 2019); thereby extending the scope of current hyper-resolution hydrological models beyond the continental scale (Hoch et al., 2023). In this novel implementation of PCR-GLOBWB, a new downscaling procedure that better incorporates fine-scale topographic climate drivers are included. In addition this implementation incorporates a snow module capable of lateral movement of frozen water resembling glaciers, which is pertinent at higher resolutions. We compare this global 30 arc-seconds simulation to previously published 5 arc-minutes and 30 arc-minutes versions of PCR-GLOBWB by evaluating simulated river discharge, snow cover, soil moisture, land surface evaporation, and groundwater storage against observation. We focus on how the model represents the hydrological cycle across scales and aim to highlight where we need to focus its efforts to improve hyper-resolution hydrological modelling.

2 Methods

2.1 30 arc-seconds PCR-GLOBWB Setup and Parametrization

PCR-GLOBWB (PCR - Global Water Balance) is a global hydrological and water resources model that estimates global water stores at various resolutions. It considers both natural and human-induced factors when estimating global water stores and fluxes. The 30 arc-seconds PCR-GLOBWB implementation presented here is built upon a schematization that has previously been applied to continental Europe (Hoch et al., 2023), in such the model presented here largely follows that presented by Hoch et al. (2023), but with a significant increase in spatial expansion that now represents the entire globe. Below we highlight important similarities and key differences between the previously published version of 30 arc-seconds PCR-GLOBWB and encourage the reader to consult its original publication for details not mentioned here. In this current implementation, (i) the parallelisation approach used by the model is updated, (ii) a novel method of downscaling coarse-scale meteorological forcing to the required 30 arc-seconds resolution is incorporated, (iii) the model now allows for lateral transport of snow and ice at high elevations and (iv) and an offline spin-up strategy is implemented. Together, these four changes to the model allowed us

https://doi.org/10.5194/egusphere-2024-1025
Preprint. Discussion started: 18 April 2024

to complete a 30 arc-seconds PCR-GLOBWB simulation with a global extent by overcoming the computational hurdle whilst still maintaining enough similarity to the previously published versions so that model outputs can be compared and evaluated in a pragmatic way.

Table 1. Table of key differences between the 30 arc-minutes, 5 arc-minutes and 30 arc-seconds PCR-GLOBWB implementations.

	30 arc-minutes	5 arc-minutes	30 arc-seconds
Downscaling Procedure	No	Lapse-Rate	Climatologies
Landcover sub grid variability	Yes	Yes	No
Lateral Snow Transport	No	No	Yes
Parallelisation	No	Basin Level	Basin and sub-basin level

2.1.1 Climate Forcing Downscaling Procedure

Previously published 5 arc-minutes and 30 arc-seconds versions of PCR-GLOBWB relied on a lapse rate-centric approach to downscale meteorological forcing to the appropriate spatial resolution (Hoch et al., 2023; Sutanudjaja et al., 2011, 2018). In contrast, the current implementation relied on an alternative approach by making use of high resolution climatologies (Karger et al., 2017). The new downscaling methodology involves bilinearly interpolating the coarse-scale meteorological forcing data to the 30 arc-seconds resolution, followed by the calculation of monthly climatologies from the interpolated fields. Interpolated climatologies were then compared to monthly high resolution reference CHELSA climatologies (1981 - 2010; Karger et al. (2017); Brun et al. (2022)) to produce a set of Julian day-of-year correction factors that incorporated high resolution topographic information (Fig. 1). The high-resolution climatologies represent the years 1981 to 2010; as such the correction factors were calculated for this time period.

Downscaling Temperature

As a first step, the coarse-scale daily temperature data (1981 - 2010) was interpolated to the 30 arc-seconds resolution using a bilinear interpolation (Tas_d). Thereafter, the interpolated values were used to calculate monthly climatologies Tas_M for the years 1981 - 2010 (Eq. 1); where N is the total number of years, M is the month and i is the day of month.

$$Tas_M = \frac{1}{N} \sum_{j=m}^{N} Tas_{d_{mi}} \tag{1}$$

The interpolated monthly climatologies were then compared to the high-resolution CHELSA reference climatologies $Tas_{chelsa,M}$ using Equation 2 to obtain a set of monthly correction factors $Tas_{chelsa,M}$.

$$CF_{Tas,M} = Tas_{chelsa,M} - Tas_M \tag{2}$$

Then, to obtain a correction factor for each Julian day of the year ($CF_{Tas,doy}$), where doy) is day of year, we employed a linear interpolation on $CF_{Tas,M}$.

Downscaling Evaporation

https://doi.org/10.5194/egusphere-2024-1025
Preprint. Discussion started: 18 April 2024

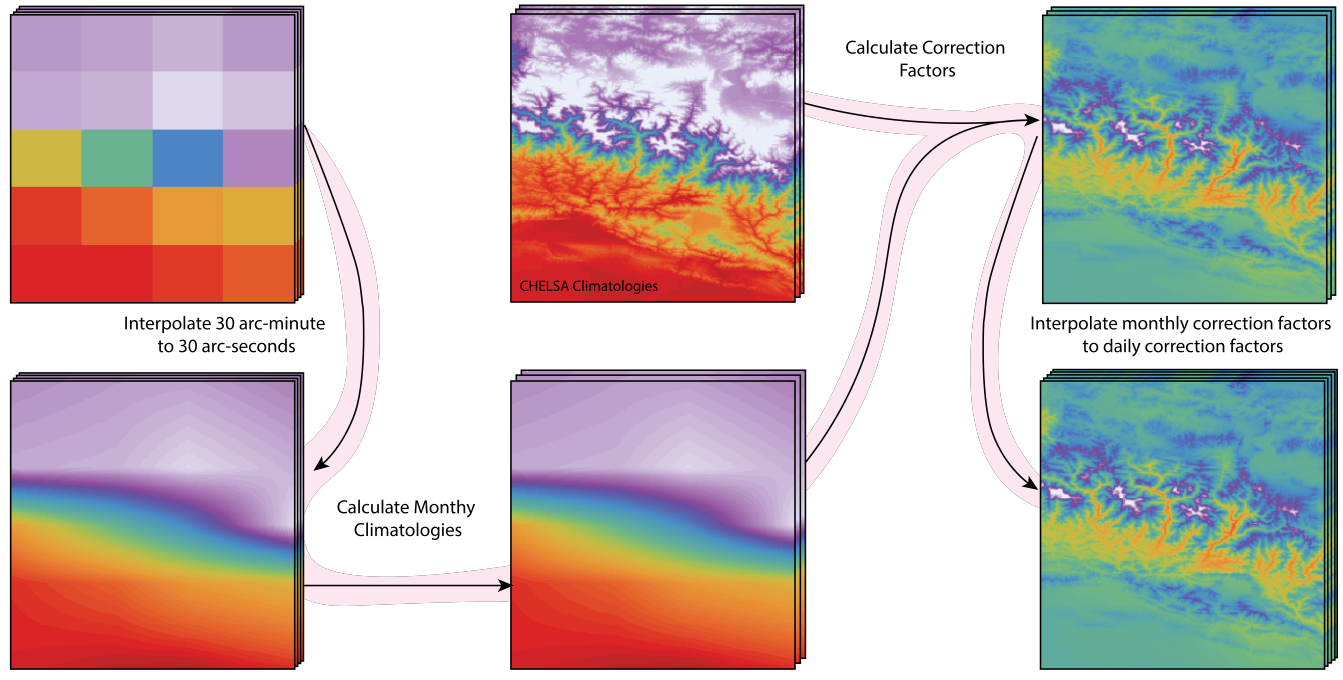

Figure 1. Procedure for downscaling meteorological forcing input date based on high resolution climatologies.

Downscaling evaporation follows the same procedure as described above for temperature; where coarse scale daily data (1981 - 2010) was interpolated to the 30 arc-seconds resolution using a bilinear interpolation ($ET_{ref,d}$) and climatologies calculated from from 1981 - 2010 (Eq. 3). Thereafter, interpolated monthly climatologies were then compared to the high resolution reference CHELSA climatologies ($CF_{ET_{ref,M}}$) using equation 4 to obtain a set of monthly climatologies and the final set of correction factor for each Julian day of the year ($CF_{ET,doy}$) was obtained through the linear interpolation of $CF_{ET_{refM}}$.

$$ET_{ref,M} = \frac{1}{N}\sum_{j=m}^{N} ET_{ref,d_{mi}} \tag{3}$$

$$CF_{ET_{ref,M}} = ET_{chelsa,M} - ET_{ref,M} \tag{4}$$

Downscaling Precipitation

As a first step, coarse-scale daily data (1981 - 2010) was interpolated to the 30 arc-seconds resolution using a bilinear interpolation (Tp_d). For the precipitation downscaling, an additional step is necessary to correct for drizzle days. Drizzle days are erroneous by-products from interpolating precipitation, which result in very light precipitation where precipitation should be zero. To account for this and remove excess precipitation, we calculated which proportion of days in each a month of the year are dry days ($dryDays$) and set that proportion of bottom values in the interpolated precipitation product to 0 (Eq. 5).

https://doi.org/10.5194/egusphere-2024-1025
Preprint. Discussion started: 18 April 2024

$$Tp_d = \begin{cases} Tp_d & \text{if } Tp_d \text{ percentile rank is > than } dryDays \\ 0 & \text{if } Tp_d \text{ percentile rank is < than } dryDays \end{cases} \quad (5)$$

Thereafter, the interpolated values are used to calculate climatologies from 1981 - 2010 (Eq. 6). The interpolated monthly climatologies were then compared to the high resolution reference climatologies using equation 7 to obtain a set of monthly climatologies.

$$Tp_M = \frac{1}{N} \sum_{j=m}^{N} Tp_{d_{mi}} \quad (6)$$

$$CF_{Tp_M} = Tp_{chelsa,M} / Tp_M \quad (7)$$

Then, to get a correction factor for each Julian day of the year ($CF_{Tp,doy}$) we employed a linear interpolation on the CF_{Tp_M}.

2.1.2 Snow and Ice transport to mimic glaciers, avalanches and wind transport

A limitation in PCR-GLOBWB highlighted by (Hoch et al., 2023) relates to how the model handles snow and ice at high elevations. Downscaled temperatures are rarely above freezing point at higher elevations and given that snowmelt is calculated using the degree day model, this results in unrealistic accumulations of frozen water. In reality excess snow and ice would be transported downslope by glaciers, avalanches and wind; however, these processes are not captured in the current version of PCR-GLOBWB. To solve this, we included a mechanism that allows lateral movement of frozen water to mimic the lateral and downslope transport of snow and ice by glaciers, avalanches and wind. The snow and ice distribution component implemented here largely follows that described by Frey and Holzmann (2015). If the snow water equivalent exceeds a threshold of (Hv = 0.625 m), lateral transport is activated. When transport is activated, the excess (i.e. transportable) volume of frozen water in a donor cell, $snow_d$, is calculated from Equation 8 and is then distributed to neighbouring down slope acceptor cells as a function of slope steepness (Eq. 9). A similar approach has previously been implemented in the community water model.(Burek et al., 2020).

$$snow_D = max(SWE - Hv, 0) * cellArea \quad (8)$$

$$snow_A = \frac{snow_D * \frac{tan(slope)}{90}}{N_{acceptorCells}} \quad (9)$$

https://doi.org/10.5194/egusphere-2024-1025
Preprint. Discussion started: 18 April 2024

2.1.3 Spin up strategy

Traditionally, to get an initial estimate of the water storage and fluxes, PCR-GLOBWB requires a mandatory spin-up period, during which the model is simulated for the first time step repetitively until the hydrological storage values (e.g., unsaturated and saturated zone) have converged to long-term steady states. However, when considering the computational resources required for a global 30 arc-seconds simulation, this approach becomes unfeasible, as especially groundwater storage would take a long time to reach equilibrium values. To overcome this obstacle, a three-phase spin-up process is implemented in the 30 arc-seconds schematization. In the first phase, PCR-GLOBWB is run for a three-year period to obtain a representative annual groundwater recharge rate Gw_{rech}. Groundwater storage is then calculated offline using Equation 10 for 1 000 iterations, where the base flow is driven by the response time of the groundwater aquifer (j). In the third and final phase, the model is run for an additional period of at least 5 years with the precalculated groundwater storage values as initial conditions to obtain the final set of initial conditions.

$$GW_{stor,i} = GW_{stor,i-1} + GW_{rech_i} - (j \times \overline{GW_{stor}} \times \frac{GW_{stor_i-1}}{\overline{GW_{stor}}})^1 \quad (10)$$

2.1.4 Parallelisation Approach

Maintaining pragmatic and feasible simulation times is a significant challenge when approaching hyper-resolutions. A simple yet effective parallelisation technique used in PCR-GLOBWB is to spatially partition the modelling domain into independent hydrological units and assign separate processors to each unit which are then completed concurrently. In the previous 5 arc-minutes PCR-GLOBWB, 53 independent spatial hydrological units were completed in parallel (Fig. 2a). This is possible because each basin's outlet ends up in a reservoir, endorheic lake, or ocean. This approach was followed in the current 30 arc-seconds implementation, where the modelling domain is split up into 215 independent hydrological units, which can be completed in parallel (Fig 2b). However, at 30 arc-seconds, for some of the larger basins in the domain, this approach still leads to extremely long simulation times if not treated further - predominantly because of the surface water routing being computationally expensive. For basin exceeding an 800 000 km^2 threshold, a hierarchical method of parallelisation was therefor used. This threshold was selected to balance efficient input/output operations and the number of point operations done by an individual processor. First, the basin is divided according to stream order so that each subbasin is smaller than the 800 000 km^2 threshold. The upper reaches of the basin are completed first and then followed by the next downstream subbasin until the last subbasin has all the necessary information (Fig 2c).

https://doi.org/10.5194/egusphere-2024-1025
Preprint. Discussion started: 18 April 2024

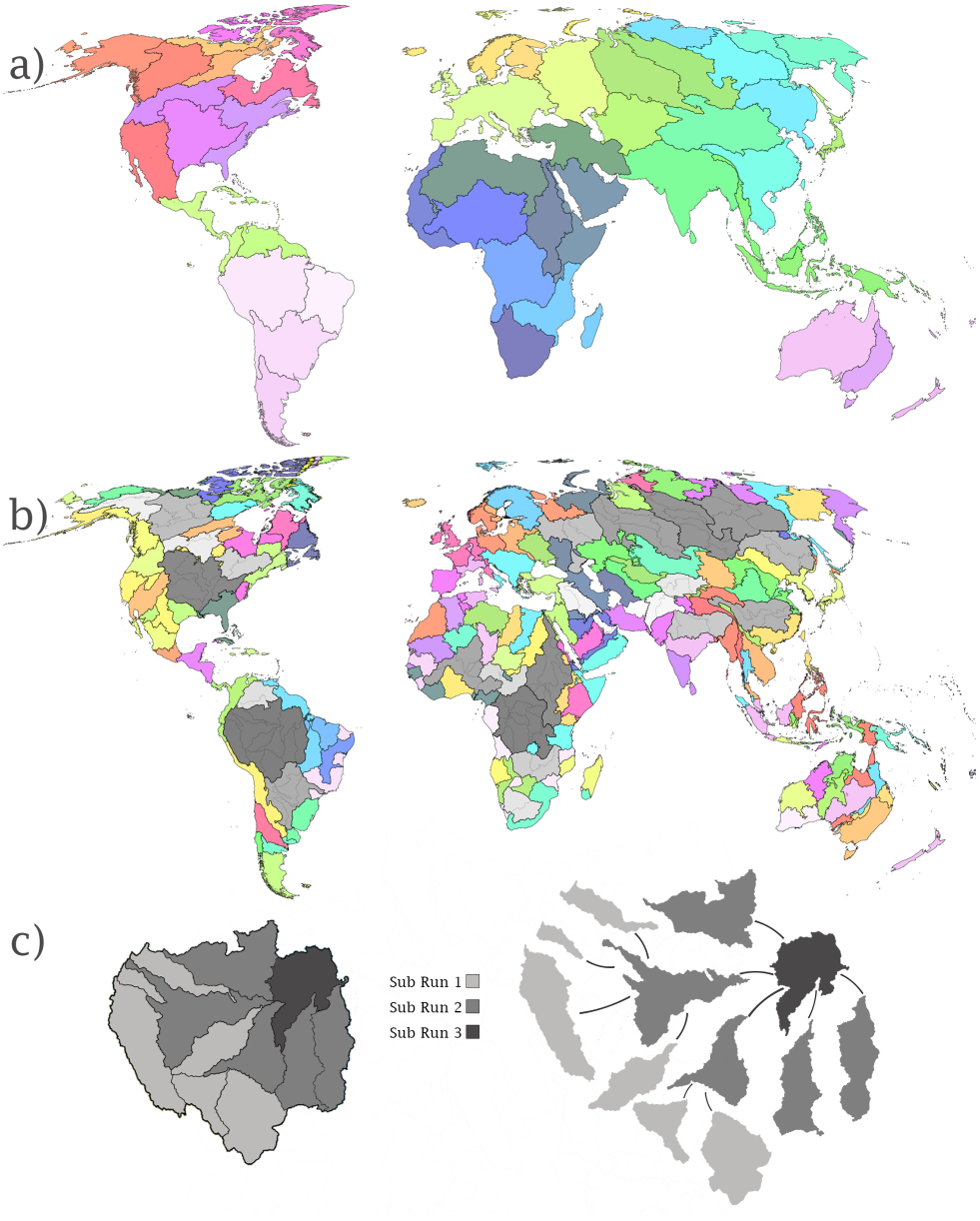

Figure 2. (a) Spatial domains used for parallelisation in the previously published 5 arc-minutes PCR-GLOBWB version and (b) the domains used for the parallelisation approach used in this 30 arc-seconds PCR-GLOBWB; which (c) requires additional subsetting and hierarchical parallelisation for basins exceeding 800 000 km^2 which are displayed in grey in sub figure b. Using the Amazon as an example, the hierarchical parallelisation involves simulating the upper sub-basins (Sub Run 1) first, followed by the intermediate sub-basins (Sub Run 2), and finally the penultimate sub-basin (Sub Run 3).

https://doi.org/10.5194/egusphere-2024-1025
Preprint. Discussion started: 18 April 2024

2.2 Global 30 arc-seconds PCR-GLOBWB simulation and evaluation

The global 30 arc-seconds parameterization described above was simulated for a multi-decadel period (1985-2019) and forced with downscaled 30 arc-minutes W5E5 temperature, precipitation, and reference potential evaporation (Lange et al., 2021). The reference potential evaporation was calculated from the Penman-Monteith formulation, following the FAO guidelines (Allen and Food and Agriculture Organization of the United Nations, 1998), using the python package pyEt (Vremec and Collenteur, 2021); input data for the calculation of the reference potential evaporation was also taken from W5E5. The initial conditions for this simulation were calculated following the three part spin-up approach described above. As the first phase, PCR-GLOBWB was run from 1979 - 1981 with hydrological states set at an initial of 0.001 m of water and 1981 was taken as the representative groundwater recharge year to calculate groundwater storage offline. The model was then put through an additional spinup period of 6 years (1979 - 1985) to get stable estimates of the other fluxes and storages. For final production, the initial conditions were used to run PCR-GLOBWB from 1985 - 2019. All simulations in this paper were run on Snellius, the Dutch National supercomputer.

To assess how capable this 30 arc-seconds PCR-GLOBWB is at reproducing the global hydrological cycle compared to coarser versions, two additional simulations were performed; one at the 5 arc-minutes and the other at the 30 arc-minutes. The same forcing and, where applicable, the same model settings were used. A spinup period of 40 years was used. For a more thorough explanation of these two models, we refer the reader to the original publications for the 30 arc-minutes (van Beek, 2008; van Beek and Bierkens, 2008; Van Beek et al., 2011) and 5 arc-minutes variants of PCR-GLOBWB (Sutanudjaja et al., 2018). All three models were simulated for the same time period, 1985 - 2019, and used the same meteorological forcing; however, key differences between the models versions are highlighted in Table 1.

2.2.1 Evaluation

To provide a more comprehensive evaluation of the global simulations, multiple hydrological variables were used for evaluation, namely total water storage, total evaporation, soil moisture, snow cover, and river discharge. To compare simulations of different resolution to one another and observation data in a fair way, we opted to evaluate the simulations at scales that matched those of the observational data. In doing so, it allowed for an assessment of the simulated values, regardless of simulation resolution whilst still allowing for comparisons between scales. As a first comparisons between the different resolutions, we also calculated the global water balance and its respective components.

Global Water Balance and Total Water Storage

In order to determine to what degree the models are able to partition water into different components of the water cycle, the global water budgets (Eq. 11) for the simulation period, 1985 - 2019, were compared. In addition, runoff/precipitation and evaporation/precipitation ratios were calculated for simulations at the three different resolutions.

$$P = E + Q + \Delta S \tag{11}$$

https://doi.org/10.5194/egusphere-2024-1025
Preprint. Discussion started: 18 April 2024

Monthly total water storage was evaluated against JPL TELLUS GRACE/GRACE-FO data for 2002 - 2019 (Kornfeld et al., 2019). The relative root mean sum of squares (RRMSE; Eq. 12 and correlation coefficient (R^2; Eq. 13) were calculated for each grid cell as an indication of how well the model was able to reproduce the temporal patterns and magnitude of total water storage anomalies. GRACE data used here are at the 30 arc-minutes resolution which is close to the Mascon solution provided in Kornfeld et al. (2019); thus 5 arc-minutes and 30 arc-seconds were aggregated to 30 arc-minutes to match the spatial resolution of GRACE by using the mean.

$$RRMSE = \frac{RMSE(obs, sim)}{\sigma(obs)} \tag{12}$$

$$R^2 = 1 - \frac{SS_{res}}{SS_{tot}} \tag{13}$$

Total Evaporation and Soil Moisture

Total evaporation and soil moisture were evaluated against station based data. Soil moisture data was obtained from the International Soil Moisture Network (Dorigo et al., 2021). In cases where more than one reading of soil moisture was taken a day, the daily mean was calculated and used for evaluation. In addition, to have a good match between the modelled soil moisture depths and the observations, only data that coincided with the depth of the first soil layer we used.

Observed total evaporation was obtained from the FLUXNET data set (Pastorello et al., 2020). The Kling-Gupta Efficiency (KGE; Eq. 14) was used to assess the accuracy of the simulated variables and for both total evaporation and soil moisture, evaluation was restricted to stations with at least 1 095 days of observation data. A value of -0.41 was used as the boundary value to determine whether the model improves upon the mean variable benchmark (Knoben et al., 2019). In addition, we analysed how the different components of the KGE score differed between resolution. Correlation coefficients (ρ) provide an overview of how well the model reproduces temporal changes in the observed data, bias ratio (β) indicates differences between the means of the simulated and observed values, and variability ratio (α) indicates how well the model replicates the variability of the observed data.

$$KGE = \sqrt{(\rho - 1)^2 + (\alpha - 1)^2 + (\beta - 1)^2} \tag{14}$$

Snow Cover

To establish to what degree the simulations were able to reproduce snow dynamics, we evaluated daily snow cover at the 30 arc-seconds resolution. For this, simulated snow water equivalent was converted into snow cover, where values greater than zeros were classified as having snow present and assigned a value of one, and values equal to zero were classified as having no snow and assigned a value of zero. The MODIS daily snow cover product (Nagler et al., 2021) was used as observation data, given the mismatch in spatial resolution between the observation data and the 30 arc-minutes and 5 arc-minutes simulations. The 5 arc-minutes and 30 arc-minutes simulated snow cover were re-gridded to the 30 arc-seconds resolution using the nearest-neighbour algorithm. As an estimate of accuracy, we calculated bias (Eq. 15), false alarm rate (FAR; Eq. 16), probability of

https://doi.org/10.5194/egusphere-2024-1025
Preprint. Discussion started: 18 April 2024

detection (POD; Eq. 17) and success ratio (SR; Eq. 18) for each grid cell in the modelling domain. The bias score indicates how well the frequency of the simulated snow cover compare to the frequency of observed snow cover; values greater than 1 indicate a tendency to overestimate the occurrence of snow on the model. POD indicates the probability of the observed snow events were correctly forecast (perfect score = 1); whereas, FAR indicates which fractions of the of the simulated snow events where incorrectly simulated since where the the observations did not have snow. The success ratio gives info on what fraction if the observed snow was correctly simulated.

$$\text{bias} = \frac{\text{hits} + \text{false alarms}}{\text{hits} + \text{misses}} \tag{15}$$

$$\text{FAR} = \frac{\text{false alarms}}{\text{correct negatives} + \text{false alarms}} \tag{16}$$

$$\text{POD} = \frac{\text{hits}}{\text{hits} + \text{misses}} \tag{17}$$

$$\text{success ratio} = \frac{\text{hits}}{\text{hits} + \text{false alarms}} \tag{18}$$

River Discharge

River discharge from the Global Runoff Data Center (GRDC) was used to evaluate river discharge simulated by PCR-GLOBWB at the three resolutions. The stations used for evaluation met the following criteria (i) 1 095 days of daily data were available and (ii) the catchment area was greater than 5 km^2. Also, to make sure that the observations locations were coupled to the right tributary, it was checked whether the catchment area reported in GRDC was similar to that of the catchment area used in the model. To enable comparisons between different resolutions, stations were selected based on the catchment area of the of 30 arc-seconds modelling domain. As the evaluation statistic, we calculated the KGE (Eq. 14) and used the value of -0.41 as the boundary value to determine whether the model improves upon the mean variable benchmark (Knoben et al., 2019).

In addition, to allow for a comparison that provides information on how the 30 arc-seconds simulation compared to the 5 arc-minutes and 30 arc-minutes simulation, the KGE skill score (Eq. 14) was calculated. This allows for inference on whether a simulation improved relative to a benchmark simulation (Towner et al., 2019). Here we assessed how the 30 arc-seconds simulations potentially improved upon the 30 arc-minutes and 5 arc-minutes simulations, where a positive value indicates an improvement and a negative value indicates a regression. To facilitate visualisation and a more intuitive comparison, the bounded variant of the KGE was used.

$$KGE_{ss} = \frac{KGE_a - KGE_{ref}}{1 - KGE_{ref}} \tag{19}$$

https://doi.org/10.5194/egusphere-2024-1025
Preprint. Discussion started: 18 April 2024

3 Results

3.1 Increased resolution: computational load and insights

Increased resolution is associated with significant increases in computational load and storage requirements (Table 2). Without parallelisation a global 5 arc-minutes and 30 arc-seconds would be impractical, with simulation times taking months. However, with the inclusion of a previously implemented basin level (Sutanudjaja et al., 2018) and the sub-basin level parallelisation scheme developed in this study, simulation times are now in the orders of days (≈ 2.5 days) for the 5 arc-minutes resolution and weeks (≈ 17 days) for the 30 arc-seconds resolution. We also find, unsurprisingly, that storage requirements increases rapidly with increased spatial resolution. For instance, writing a single variable to disk at the daily frequency results in a 2 000 fold increase in in storage requirements when moving from 30 arc-minutes to 30 arc-seconds (Table 2). Storing all possible variables will equate to 365 Gb for the 30 arc-minutes while the 30 arc-seconds resolution storage requirements approach the petabyte scale.

Increased model resolution, does However, provide a unique and improved representation of the hydrological cycle (Fig. 3). For instance, compared to the 5 arc-minutes and 30 arc-seconds resolution, the 30 arc-seconds resolution better resolves spatial patterns in soil saturation related to elevation and landcover type. In the 30 arc-seconds simulation, variations in soil saturation degree related to drainage networks become visible. When comparing the resolutions over the Himalayas, the 30 arc-second simulation represents a continuous field and does not display the footprint of the original coarse scale meteorological forcing as is present in the 5 arc-minute resolution (Fig. 3). In addition, when shifting focus towards the Taihang mountains in mainland China, the difference between the arid Gobi towards the west and humid forests towards the east is most evident in the 30 arc-second simulation (Fig. 3).

Table 2. Overview on the computational and storage requirements for a multi-decadel global PCR-GLOBWB simulation at different resolutions 30 arc-minutes, 5 arc-minutes and 30 arc-seconds resolutions

Resolution	Serial Simulation Time (hrs)	Parallel Simulation Time (hrs)	Storage (GB; min - max)
30 arc-minute	43	NA	3.3 - 365
5 arc-minute	2 465	66	182 - 20 748
30 arc-seconds	39 245	401	8 200 - 934 800

https://doi.org/10.5194/egusphere-2024-1025
Preprint. Discussion started: 18 April 2024

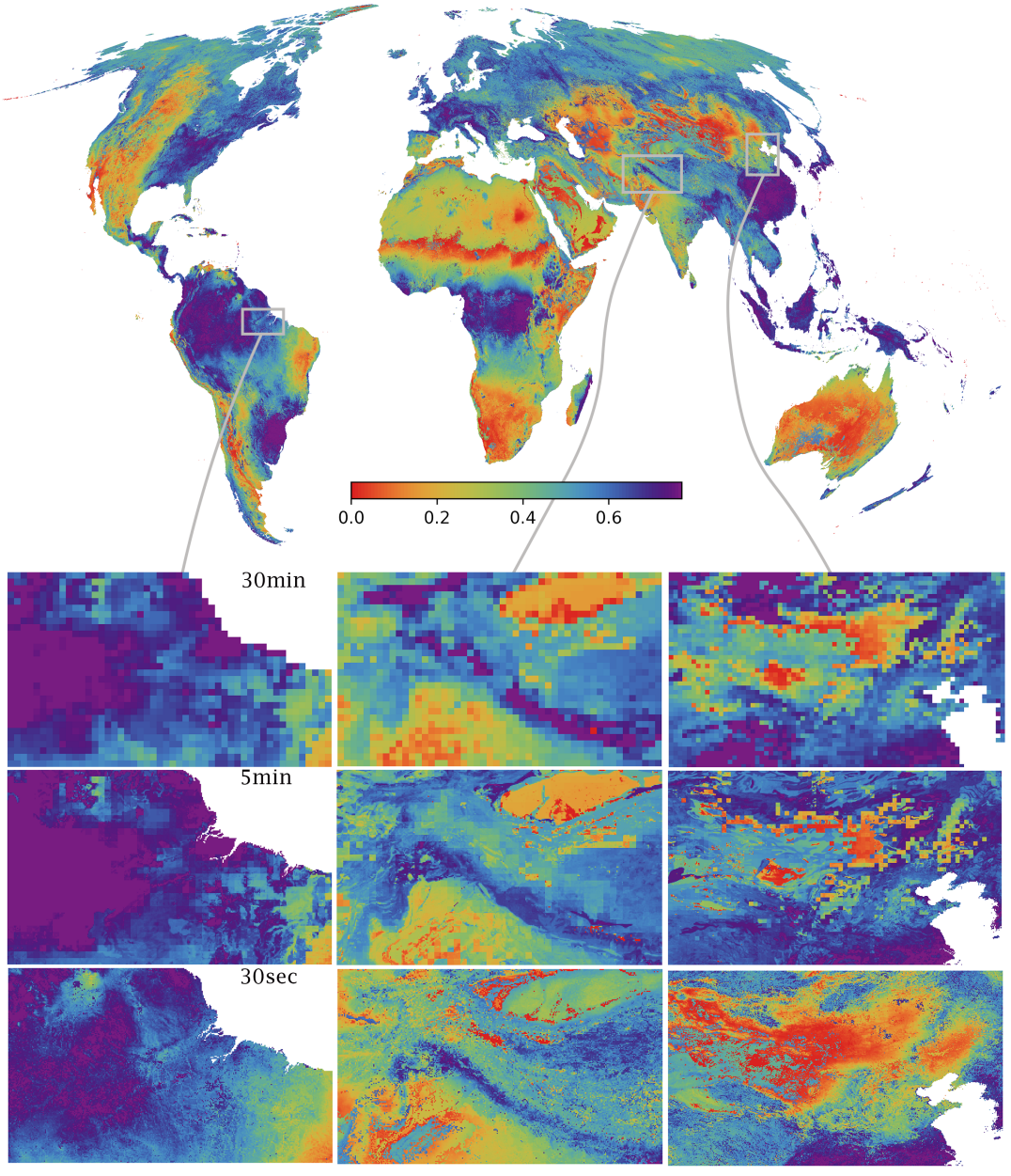

Figure 3. Mean (1985 - 2019) upper soil saturation (-) simulated by PCR-GLOBWB at 30 arc-seconds resolution. Zoomed insets compare how the highlighted regions differ between the 30 arc-seconds, 5 arc-minutes and 30 arc-minutes resolution PCR-GLOBWB simulations.

https://doi.org/10.5194/egusphere-2024-1025
Preprint. Discussion started: 18 April 2024

3.2 Global Water Balance and Total water storage

Table 3. Global water balance components $km^3 year^{-1}$ for 1985 - 2019 for a 30 arc-minutes, 5 arc-minutes, and 30 arc-seconds simulated by PCR-GLOBWB.

Simulation	Precipitation	Evaporation	Runoff	Storage
30 arc-minutes	112 140	64 091	47 089	960
5 arc-minutes	112 159	63 277	49 223	-341
30 arc-seconds	121 798	84 275	39 605	-2 082

To evaluate the impact of increasing the spatial resolution on the representation of the global water cycle, we studied the long-term differences in the global water balance components. For this comparison we focus on relative values since the absolute values in precipitation differ due to differences in simulated land area and downscaling methodology. For the 30 arc-minutes and 5 arc-minutes the results are comparable; However,when considering the 30 arc-seconds simulation, the relative evaporation rates are significantly higher and runoff significantly lower compared to the other two simulations (Table 1). As resolution increases, there is a decrease in the relative amount of precipitated water accumulating as runoff, which is due to the increase in relative rates of evaporation 4).

https://doi.org/10.5194/egusphere-2024-1025
Preprint. Discussion started: 18 April 2024

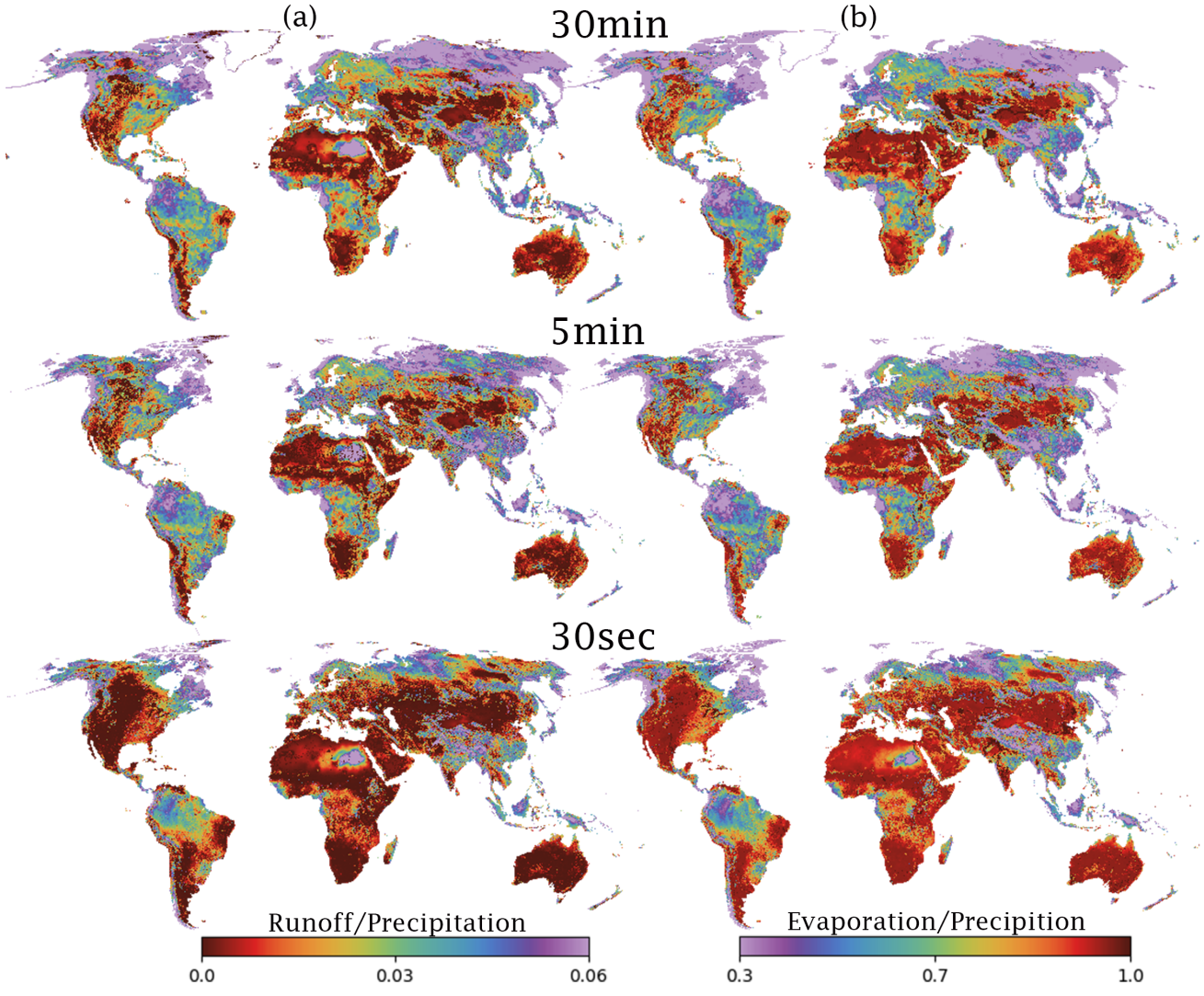

Figure 4. Mean annual mean (a) Runoff/Precipitation and (b) Evaporation/Precipitation ratios for a 30 arc-minutes, 5 arc-minutes, and 30 arc-seconds simulated by PCR-GLOBWB from 1985 - 2019.

290 The simulated total water storage changes are comparable between the three resolutions. When comparing the total water storage the GRACE satellite observations. We find that in terms of temporal dynamics, the 5 arc-minutes resolution best resembles the GRACE data; followed by the 30 arc-minutes and 30 arc-seconds resolutions (Fig. 5a). The RRMSE between the modelled and observed anomalies in total water storage are similar for all three resolutions, with on average a slightly better RRMSE for the 30 arc-seconds simulations is reported (Fig. 5b)

https://doi.org/10.5194/egusphere-2024-1025
Preprint. Discussion started: 18 April 2024

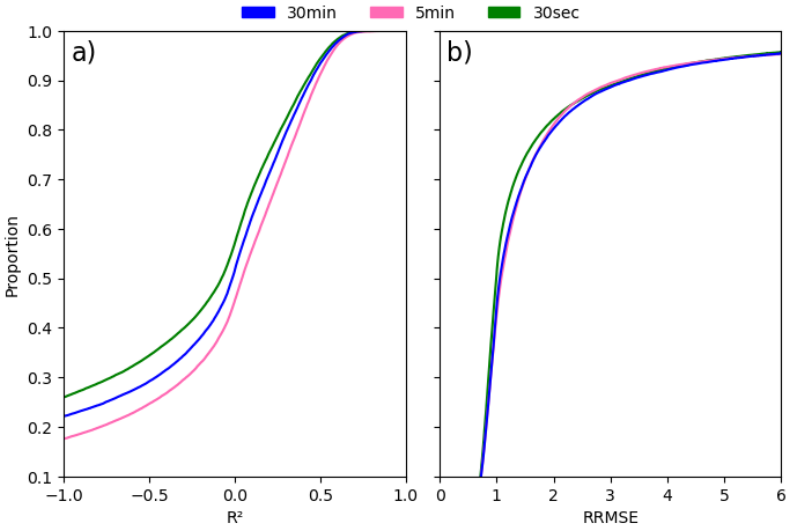

Figure 5. (a) $R^2$and (b) RRMSE for simulated Total Water Storage compared to GRACE data for 2002 - 2019.

3.3 Soil Moisture and Total Evaporation

Simulated soil moisture is indistinguishable between the 30 arc-minutes, 5 arc-minutes and 30 arc-seconds simulations; 50% of 1 676 stations (Fig. A1) that display a KGE greater than -0.41 (Fig. 6a). Interestingly, when considering the different components of KGE differences emerge; as resolution increases the correlation and variability increases yet this is offset by a reduction in bias (Fig. 6b,c,d). In contrast, total evaporation displays significant differences between the 30 arc-seconds simulation in comparison to the 5 arc-minutes and 30 arc-minutes simulation; whereas evaporation for the 30 arc-minutes and 5 arc-minutes are similar. Only 85% of the 143 stations (Fig. A2) display a KGE greater than -0.41 for the 30 arc-seconds resolution; whereas, almost all of the stations in the 30 and 5 arc-minutes simulation exceeded this threshold (Fig. 6e). This difference is attributable to a reduction in correlation for the 30 arc-seconds (Fig. 6f) and an overestimation of the mean (Fig. 6g) and variance (Fig. 6h) of the simulated evaporation compared to observations.

https://doi.org/10.5194/egusphere-2024-1025
Preprint. Discussion started: 18 April 2024

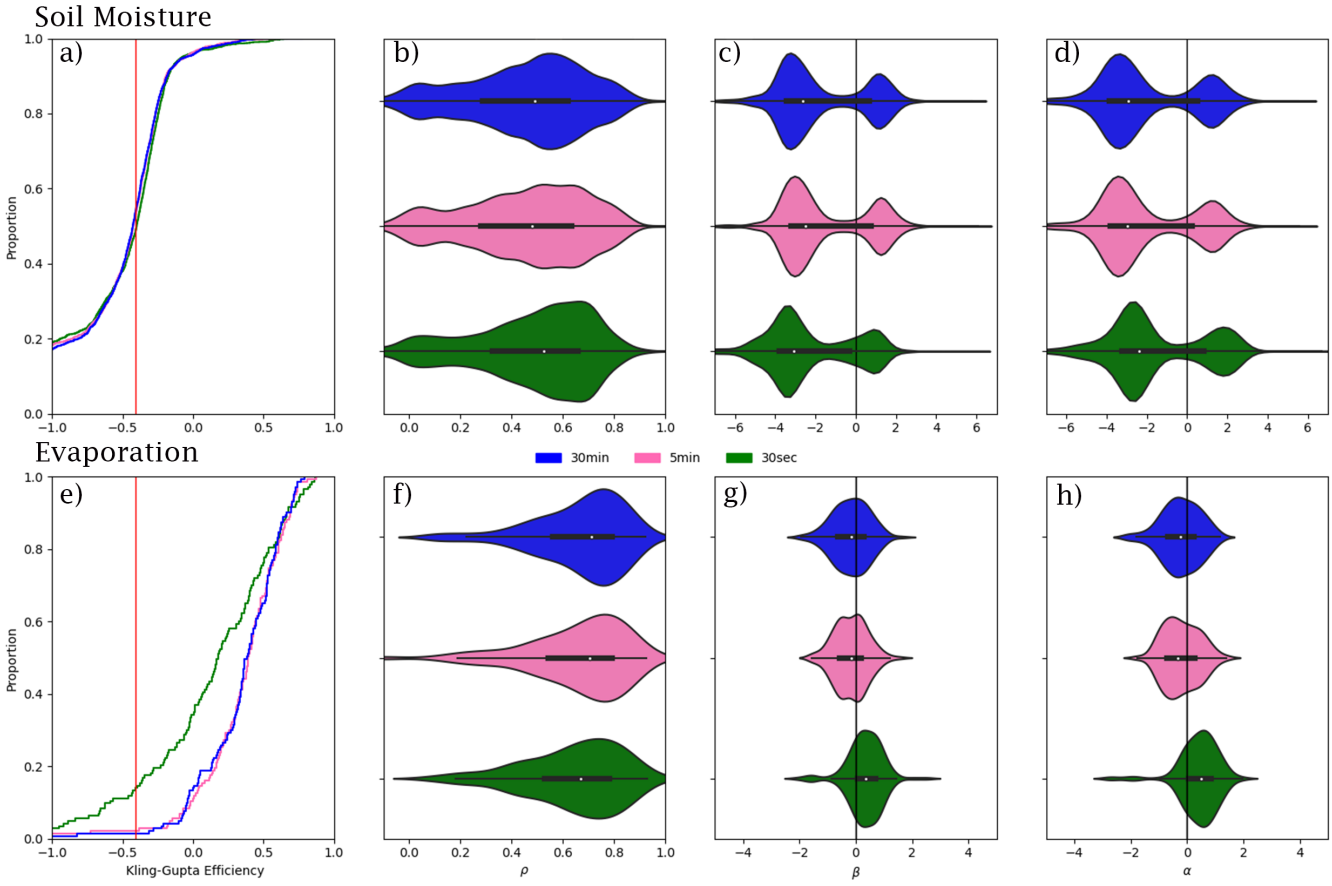

Figure 6. Top: Soil Moisture (a) KGE and associated constituents of KGE: (b) correlation, (c) beta, (d) alpha from the ISMN. Bottom: Total Evaporation (e) KGE and associated constituents of KGE: (f) correlation, (g) beta, (h) alpha from FLUXNET. Values greater than -0.41 (red line) indicate the value at which stations improves upon the mean flow benchmark.

3.4 Snow Cover

Table 4. Contingency table for observed and simulated snow cover.

		Observed					
		True			False		
		30 arc-minutes	5 arc-minutes	30 arc-seconds	30 arc-minutes	5 arc-minutes	30 arc-seconds
Simulated	True	0.14	0.13	0.14	0.030	0.023	0.024
	False	0.011	0.015	0.013	0.82	0.83	0.82

https://doi.org/10.5194/egusphere-2024-1025
Preprint. Discussion started: 18 April 2024

Table 5. Bias, False Alarm Rate (FAR), Probability of Detection (POD) and Success Rate (SR) for snow cover at 30 arc-minutes, 5 arc-minutes and 30 arc-seconds simulated by PCR-GLOBWB.

	Bias	FAR	POD	SR
30 arc-minutes	1.13	0.035	0.93	0.82
5 arc-minutes	1.05	0.027	0.90	0.85
30 arc-seconds	1.07	0.028	0.92	0.85

The inclusion of the lateral movement of frozen water through glaciers, avalanches or wind resulted in a more accurate accumulation and redistribution of frozen water at high elevation and prevented the erroneous accumulation of frozen water into snow towers. When evaluated against observed snow cover, all three the resolutions tended to overestimate the frequency of snow cover. Both the 30 arc-seconds and 5 arc-minutes showed lower positive bias compared to the 30 arc-minutes simulation (Table 4). The 30 arc-minutes simulation displays a higher false alarm rate and shows an increased tendency to simulate snow on occasions where there is no snow present (Table 5). With a higher POD the 30 arc-seconds and 30 arc-minutes shows a similar ability to correctly simulate occasions where snow is present, in contrast to the 5 arc-minutes simulation (Table 5). The 30 arc-seconds and 5 arc-minutes displays similar success ratios whilst the 30 arc-minutes is less successful.

https://doi.org/10.5194/egusphere-2024-1025
Preprint. Discussion started: 18 April 2024

3.5 River Discharge

Simulated river discharge more closely resembles the observations in the 30 arc-seconds resolution with close to 80% of the 7 086 stations showing skilful discharge simulations when compared to the 5 arc-minutes (70%) and the 30 arc-minutes (30%, Fig. 7a). The improvement in the 30 arc-second simulations is mainly brought about by increases in the correlation values and reductions in the bias and variance errors (Fig. 7b,c,d). The 30 arc-seconds simulation improves upon the 30 arc-minutes and 5 arc-minutes simulation in the majority of locations and this improvement is more pronounced for smaller catchments compared to larger catchments (Fig. 8).

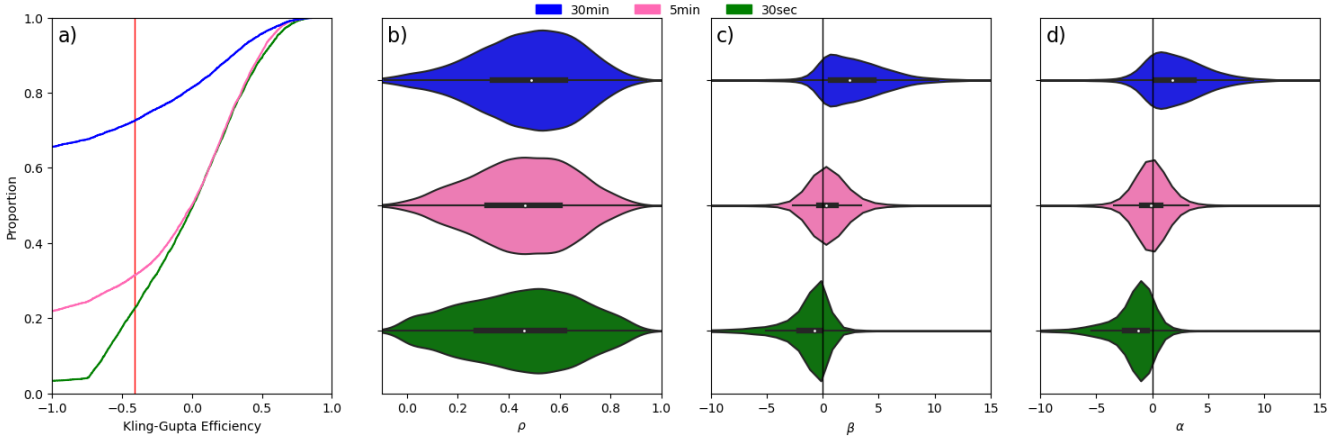

Figure 7. (a) KGE, (b) correlation component, (c) beta component, (d) alpha component calculated for daily river discharge from a 30 arc-minutes, 5 arc-minutes and 30 arc-seconds global PCR-GLOBWB simulation from 1985 - 2019. Values greater than -0.41 (red line) indicate the value at which stations improves upon the mean flow benchmark.

https://doi.org/10.5194/egusphere-2024-1025
Preprint. Discussion started: 18 April 2024

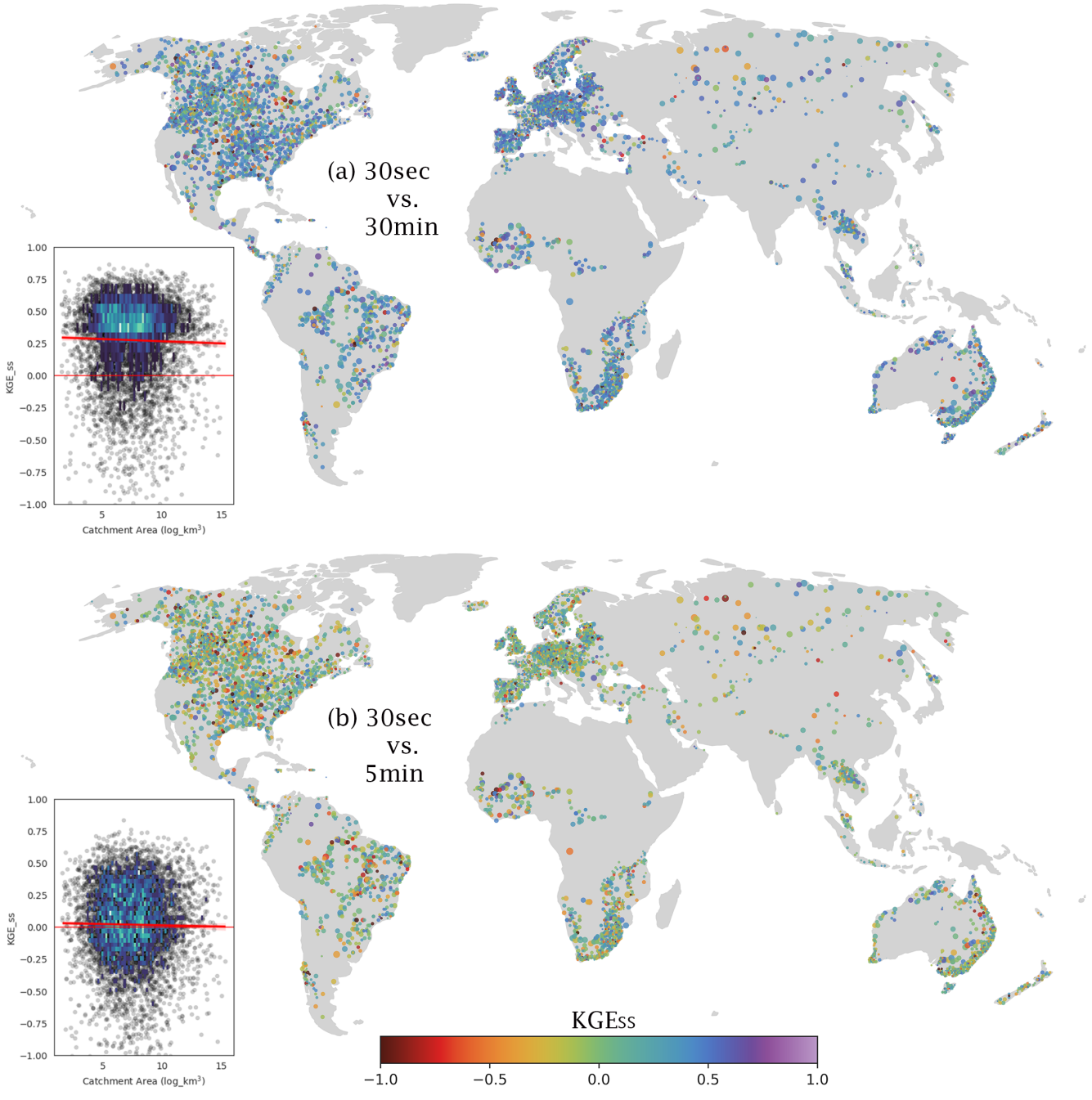

Figure 8. Spatial distribution of improvements in KGE skill score for (a) 30 arc-seconds vs 30 arc-minutes (b) 30 arc-seconds vs 5 arc-minutes. Panel plots show the relationship between catchment size and KGE skill score; green to purple colours entail a higher KGE with higher resolution.

https://doi.org/10.5194/egusphere-2024-1025
Preprint. Discussion started: 18 April 2024

4 Discussion

4.1 Computational and Storage demands

We show here that truly global hyper-resolution modelling is indeed possible with today's computational resources. However, long simulation times and excessive storage requirements for such simulations will hinder the reproducibility and accessibility for the wider hydrological community. Future attempts should consider how newer technologies such as graphical processing units or using alternative methods of parallelisation like asynchronous many tasks which could help to solve these problems and reduce simulation times (Freitas et al., 2022; de Jong et al., 2022). An important motivation for the development of global hyper-resolution models is that they are to be used in climate change studies (Wada et al., 2017); yet the storage and computational requirements for such an endeavour are still a limiting factor. To illustrate, here we evaluate four variables at a daily and one variable at the monthly frequency, which requires approximately 27 terabytes of storage. To obtain a more comprehensive view on the hydrological cycle, it would be preferable to have daily frequency data for more of the available model outputs. When considering all possible model outputs (114 variables) - this would yield a storage load of approximately one petabyte for a 35-year simulation. Extending this approach for a multi-model future simulation using the CMIP6 ensemble (approximately 130 models) storage requirements are estimated at 780 petabytes. Petascale storage requirements are inaccessible - or at the very least impractical - for most of the hydrological community. However, expected simulation times are less daunting, total simulation time would approach three months on the Dutch National Super Computer. Although this would provide valuable information, it also means that hydrology is now faced with the same issues current GCM's face; that is that although such simulations are possible, data storage becomes a limitation (Schär et al., 2020). While solutions to the computational and storage limitations remain elusive; leveraging the recent trend towards cloud technologies for storing and disseminating earth science data is promising, yet the costs of these services remain high (Beven et al., 2015). Moreover, hyper-resolution physical based models may also benefit from adopting similar model deployment and dissemination strategies which are common amongst the machine learning community. For example, making intermediary states (ie., yearly states) available to the public could allow for more of the community to reproduce their required model outputs on the hardware available to them.

4.2 Increasing resolution and model accuracy

By increasing the model resolution we should expect to have a better representation of hydrological systems. However, we report mixed success when looking at the reproductions of different variables; below we discuss each of the evaluated variables.

Global Water Budget and Total Water Storage

Total water storage anomalies did not respond drastically to increasing model resolution, yet there were small reductions in the magnitude of error as modelling resolution is increased. This may be related to a more realistic distribution of water across the landscape at finer resolutions. Yet correlations were worse for the 30 arc-seconds, followed by the 30 arc-minutes and best for the 5 arc-minutes simulation. However, it is also important to note that benefits of higher resolutions may not be captured when using GRACE data to evaluate since the original resolution is at 30 arc-minutes and thus might by itself also capture a different signature than produced by the high-resolution simulations (Hoch et al., 2023). Partitioning between the major water reserves

https://doi.org/10.5194/egusphere-2024-1025
Preprint. Discussion started: 18 April 2024

differed in response to increasing model resolution, with a markedly larger value of evaporation and lower discharge at the highest resolution. In comparison to other global models the 30 arc-seconds PCR-GLOBWB rates of evaporation are within previously reported ranges (60 000 - 85 000 $km^3 year^{-1}$) whereas runoff is slightly lower than previously reported (42 000 - 66 000 $km^3 year^{-1}$; Haddeland et al. (2011)). Interestingly, runoff is inline with a machine learning based estimate based off of station based river discharge data (Ghiggi et al., 2019). Expected evaporation to precipitation ratios are around 60% (Miralles et al., 2011), and for the 30 arc-minutes (57%) and 5 arc-minutes (56%) simulations this is the case. However, for the 30 arc-seconds resolution the evaporation to precipitation ratios is 69%, thus exceeding the expected value by approximately 9 percentage points.

Snow Cover

Increasing resolution resulted in better spatial representation of snow cover, with the highest resolution presenting the highest accuracy, although differences are small. These improvements could be related to both increasing modelling resolution or the introduction of lateral snow transport which prevents the formation of erroneous snow towers. Although not the direct focus of this work, future studies should look at how snow can be better represented in global hydrological models by including process that are important in determining the water dynamics in ice and snow, especially when modelling at fine spatial resolutions. For instance, the current PCR-GLOBWB does not have unique glacier implementations. Yet, glaciers have been shown to locally and regionally important and including such processes do results in better predictions at larger scales (Hanus et al., 2024; Wiersma et al., 2022). Similarly, work needs to be done to improve snow dynamics and move beyond the simple snow melt model present in the model by including additionally processes which have also been shown to increase accuracy of predictions (Freudiger et al., 2017).

Soil Moisture and Evaporation

Overall, predictions of soil moisture did not show much improvement as resolution increased. Evaporation results at the 30 arc-seconds are significantly worse than those of the lower resolutions. It is difficult to put a finger on the precise cause of this result. Since, soil moisture estimates are similar between resolutions, it is feasibly due to difference in the meteorological forcing or the parameterization of the evaporation reduction in relation to soil moisture that is responsible. As shown hereafter in section 4.3, it is most likely the parameterization.

River Discharge

Predictions of river discharge improved markedly as modelling resolution increased. 30 arc-seconds displayed the most accurate predictions of river discharge. For the 30 arc-minutes and 5 arc-minutes resolution the model tended to overestimate river discharge, whilst the 30 arc-seconds results are underestimated. The improvement in KGE values at higher resolution is mostly the result of a better timing of the discharge peaks and troughs resulting in larger correlation coefficients (Fig. 8). A positive result from these evaluations is that smaller catchments are now better represented by the model, a result directly related to increased model resolution. Increased resolutions are known to better represent smaller catchments (Hoch et al., 2023; O'Neill et al., 2021; Aerts et al., 2022).

https://doi.org/10.5194/egusphere-2024-1025
Preprint. Discussion started: 18 April 2024

4.3 Untangling Model Scaling and Forcing Downscaling Affects

Table 6. Water balance components $km^3 year^{-1}$ for 1985 - 2019 for a 30 arc-minutes, 5 arc-minutes, and 30 arc-seconds simulated by PCR-GLOBWB over the European Continent.

Resolution	Downscaling	Precipitation	Evaporation	Runoff	Storage
5 arc-minutes	Old	6 532	3 601	2 804	127
	New	6 937	4 002	2 807	127
30 arc-seconds	Old	6 377	4 468	1 860	49
	New	6 779	4 947	1 787	44

In order to differentiate between the effects of the new downscaling methodology and those related to model parameterisation, the 5 arc-minutes and 30 arc-seconds simulations, using the old and new downscaling method, were compared over continental Europe and evaluated as above (Table 6 & Fig. 9). The facts that the new downscaling method provides comparable results when comparing it to the old downscaling method at the same resolution, suggests that the differences in the model results are most likely attributable to model parameterisation. One likely candidate is the way in which landcover is handled within the model at the 30 arc-second resolution. For the 30 arc-minute and 5 arc-minute models, PCR-GLOBWB allows for sub-grid variability in landcover type, where as in the 30 arc-seconds only the dominant landcover type is assumed per grid cell. This was done to save computation time by avoiding having to loop over land cover classes for each time step. Since forest is often the predominant type, even in agricultural landscapes, and forests generally have higher evaporation than crops, evaporation is likely overestimated. Landcover representation has been shown to be important at kilometre and even sub-kilometre resolution (Singh et al., 2015; Lazin et al., 2020). Our results suggest that global hydrological models need to incorporate landcover heterogeneity even at kilometre scale in search of better predictive capacity, However, global landcover dataset are the sub-kilometre resolution (Singh et al., 2015), which will result in larger computation demands.

https://doi.org/10.5194/egusphere-2024-1025
Preprint. Discussion started: 18 April 2024

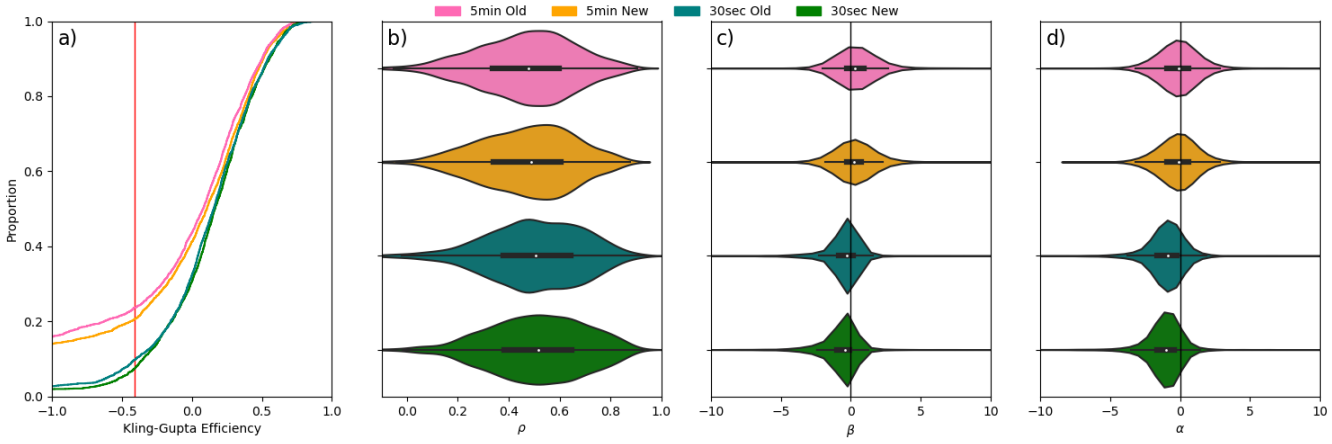

Figure 9. (a) KGE, (b) correlation component, (c) beta component, (d) alpha component calculated for daily river discharge from a 30 arc-minutes, 5 arc-minutes and 30 arc-seconds PCR-GLOBWB simulation from 1985 - 2019 for the European region. Values greater than -0.41 (red line) indicate the value at which stations improves upon the mean flow benchmark.

4.4 Global Hyper-resolution hydrological modelling: status and recommendations

Our work advances global hyper-resolution modelling and its application beyond the continental scale (Hoch et al., 2023; O'Neill et al., 2021; Vergopolan et al., 2021; Chaney et al., 2021). We show that a hyper-resolution global hydrological model is feasible given the computational limits currently in place. However, it also highlights that storage is expected to become a significant challenge as global hydrological modelling advances. This will create additional challenges when output data are used for further analysis and when extracting point location time series in a computationally effective way.

The introduction of the climatology-centred downscaling method and ability to move frozen water stores laterally result in more continuous and ultimately a more realistic representation of the hydrological cycle. Hoch et al. (2023) proposed that enhancing the representation of additional physical processes at the kilometre scale could enhance the predictions. The findings presented in this study indicate that this is indeed true, although further efforts are required to further enhance the predictive capabilities. Furthermore, as also shown by (Hoch et al., 2023) there are a number of epistemic uncertainty issues related to global hydrological modelling that still need to be addressed. For instance we need a better representation of the land surface processes, snow and ice processes as these processes play a dominant role at fine spatial resolution and can no longer be neglected or captured in existing conceptual parametrization. Another important issue that needs to be addressed is obtaining high-resolution climate forcings. At finer spatial resolution altitude effects start to play a key role in precipitation totals, snow and ice formation, melt and evaporation and thus require fine resolution meteorological information if possible at the global scale.

On the other hand, moving to a higher resolution allows for a better match with in situ observations and more recently released high resolution remote sensing products. The importance of scale commensurability between model outputs and that

https://doi.org/10.5194/egusphere-2024-1025
Preprint. Discussion started: 18 April 2024

of in situ observations has been highlighted (Beven et al., 2022). For instance, the caravan dataset which has 6 830 stations for small river catchments (Kratzert et al., 2023), could be used to better underpin the accuracy of simulated river discharge values at higher resolution. As has been done for smaller scale studies (Aerts et al., 2023). Resolutions coarser than 30 arc-seconds would not allow for the inclusion of these river catchments, given the disconnect between modelling resolution and observed data station sizes. In addition, high resolution soil moisture data from Sentinal ESA-CCI will also be a valuable resource for evaluating hyper-resolution simulations once their time series are long enough.

5 Conclusions

The main goal of this study was to develop a unique global hyper-resolution hydrological model that covers a period of several decades (1985 – 2019), expanding the current hyper-resolution hydrological models beyond continental boundaries. We incorporated a novel downscaling approach and lateral movement of frozen water that ultimately yields more realistic representations of the hydrological cycle. Yet, as resolution increased the model tended to over-estimate rates of total evaporation which resulted in reductions in runoff. This suggests that additional processes that are relevant at the hyper resolution need further attention. Overall, the pursuit of hyper-resolution hydrological models are driven by the assumption that they will be able to provide stake-holders with more local estimates of water resources; one promising result that supports this notion is that as resolution increased the the accuracy of river discharge also increased.

https://doi.org/10.5194/egusphere-2024-1025
Preprint. Discussion started: 18 April 2024

Appendix A: Appendix

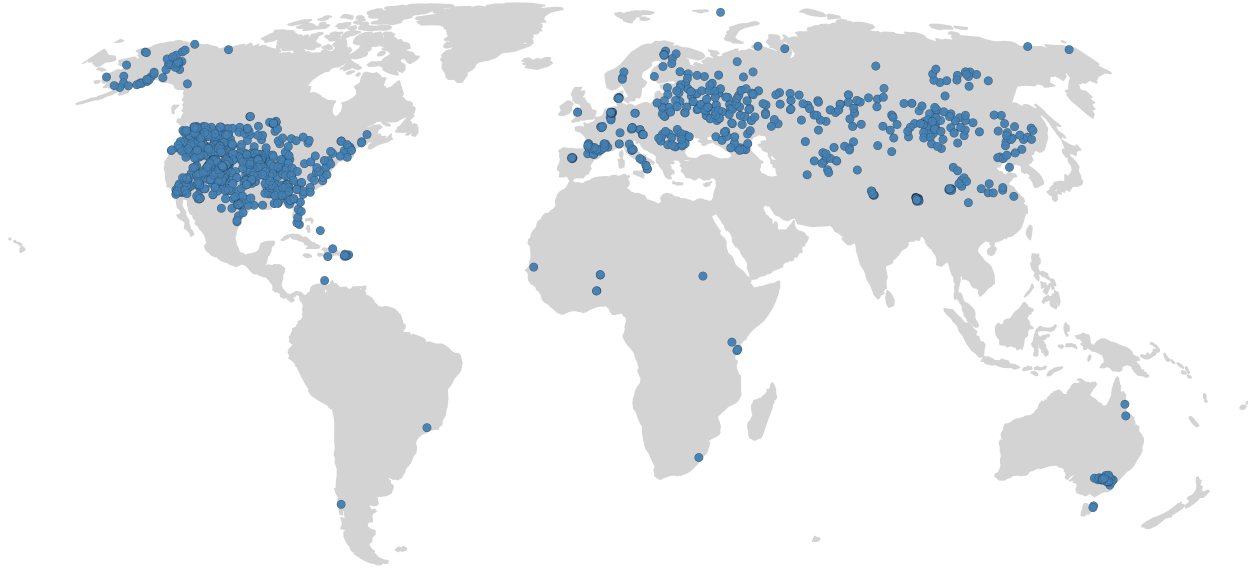

Figure A1. Map showing locations of stations used for validation of simulated soil moisture.

Figure A2. Map showing locations of stations used for validation of simulated total evaporation.

https://doi.org/10.5194/egusphere-2024-1025
Preprint. Discussion started: 18 April 2024

Author contributions. **BvJ:** Data curation, Formal analysis, Software, Validation, Visualization, Writing – original draft preparation. **NW:** Conceptualization, Formal analysis, Project administration, Resources, Supervision, Writing – review & editing. **ES:** Conceptualization, Data curation, Software, Writing – review & editing. **JH:** Data curation, Software, Validation, Writing – review & editing. **BD:** Data curation, Software, Validation, Writing – review & editing. **JJ:** Formal analysis, Software, Writing – review & editing. **RvB:** Conceptualization, Data curation, Writing – review & editing. **MB:** Conceptualization, Funding acquisition, Project administration, Resources, Supervision, Writing – review & editing.

Competing interests. The authors have also no other competing interests to declare.

Acknowledgements. This work made use of the Dutch national e-infrastructure with the support of the SURF Cooperative (using grant no. EINF-4875 & EINF-6855). MB acknowledges support from the ERC Advanced 969 Grant scheme (Grant no. 101019185 – GEOWAT). Some data and model parametrization stems from work done as part of the Climate-KIC project "Agriculture Resilient, Inclusive, and Sustainable Enterprise (ARISE)".

https://doi.org/10.5194/egusphere-2024-1025
Preprint. Discussion started: 18 April 2024

References

Aerts, J. P. M., Hut, R. W., van de Giesen, N. C., Drost, N., van Verseveld, W. J., Weerts, A. H., and Hazenberg, P.: Large-sample assessment of varying spatial resolution on the streamflow estimates of the wflow_sbm hydrological model, Hydrology and Earth System Sciences, 26, 4407–4430, https://doi.org/10.5194/hess-26-4407-2022, 2022.

Aerts, J. P. M., Hoch, J. M., Coxon, G., van de Giesen, N. C., and Hut, R. W.: On the importance of observation uncertainty when evaluating and comparing models: a hydrological example, EGUsphere, pp. 1–26, https://doi.org/10.5194/egusphere-2023-1156, 2023.

Alcamo, J.: Water quality and its interlinkages with the Sustainable Development Goals, Current Opinion in Environmental Sustainability, 36, 126–140, https://doi.org/10.1016/j.cosust.2018.11.005, 2019.

Allen, R. G. and Food and Agriculture Organization of the United Nations, eds.: Crop evapotranspiration: guidelines for computing crop water requirements, no. 56 in FAO irrigation and drainage paper, Food and Agriculture Organization of the United Nations, Rome, ISBN 9789251042199, 1998.

Benedict, I., van Heerwaarden, C. C., Weerts, A. H., and Hazeleger, W.: The benefits of spatial resolution increase in global simulations of the hydrological cycle evaluated for the Rhine and Mississippi basins, Hydrology and Earth System Sciences, 23, 1779–1800, https://doi.org/10.5194/hess-23-1779-2019, 2019.

Beven, K., Cloke, H., Pappenberger, F., Lamb, R., and Hunter, N.: Hyperresolution information and hyperresolution ignorance in modelling the hydrology of the land surface, Science China Earth Sciences, 58, 25–35, https://doi.org/10.1007/s11430-014-5003-4, 2015.

Beven, K., Lane, S., Page, T., Kretzschmar, A., Hankin, B., Smith, P., and Chappell, N.: On (in)validating environmental models. 2. Implementation of a Turing-like test to modelling hydrological processes, Hydrological Processes, 36, e14 703, https://doi.org/10.1002/hyp.14703, 2022.

Bierkens, M. F. P.: Global hydrology 2015: State, trends, and directions, Water Resources Research, 51, 4923–4947, https://doi.org/10.1002/2015WR017173, 2015.

Bierkens, M. F. P., Bell, V. A., Burek, P., Chaney, N., Condon, L. E., David, C. H., De Roo, A., Döll, P., Drost, N., Famiglietti, J. S., Flörke, M., Gochis, D. J., Houser, P., Hut, R., Keune, J., Kollet, S., Maxwell, R. M., Reager, J. T., Samaniego, L., Sudicky, E., Sutanudjaja, E. H., Van De Giesen, N., Winsemius, H., and Wood, E. F.: Hyper-resolution global hydrological modelling: what is next?: "Everywhere and locally relevant", Hydrological Processes, 29, 310–320, https://doi.org/10.1002/hyp.10391, 2015.

Brun, P., Zimmermann, N. E., Hari, C., Pellissier, L., and Karger, D. N.: CHELSA-BIOCLIM+ A novel set of global climate-related predictors at kilometre-resolution, https://doi.org/10.16904/ENVIDAT.332, 2022.

Burek, P., Satoh, Y., Kahil, T., Tang, T., Greve, P., Smilovic, M., Guillaumot, L., Zhao, F., and Wada, Y.: Development of the Community Water Model (CWatM v1.04) – a high-resolution hydrological model for global and regional assessment of integrated water resources management, Geoscientific Model Development, 13, 3267–3298, https://doi.org/10.5194/gmd-13-3267-2020, 2020.

Chaney, N. W., Torres-Rojas, L., Vergopolan, N., and Fisher, C. K.: HydroBlocks v0.2: enabling a field-scale two-way coupling between the land surface and river networks in Earth system models, Geoscientific Model Development, 14, 6813–6832, https://doi.org/10.5194/gmd-14-6813-2021, 2021.

de Jong, K., Panja, D., Karssenberg, D., and van Kreveld, M.: Scalability and composability of flow accumulation algorithms based on asynchronous many-tasks, Computers & Geosciences, 162, 105 083, https://doi.org/10.1016/j.cageo.2022.105083, 2022.

Dorigo, W., Himmelbauer, I., Aberer, D., Schremmer, L., Petrakovic, I., Zappa, L., Preimesberger, W., Xaver, A., Annor, F., Ardö, J., Baldocchi, D., Bitelli, M., Blöschl, G., Bogena, H., Brocca, L., Calvet, J.-C., Camarero, J. J., Capello, G., Choi, M., Cosh, M. C., van de

https://doi.org/10.5194/egusphere-2024-1025
Preprint. Discussion started: 18 April 2024

Giesen, N., Hajdu, I., Ikonen, J., Jensen, K. H., Kanniah, K. D., de Kat, I., Kirchengast, G., Kumar Rai, P., Kyrouac, J., Larson, K., Liu, S., Loew, A., Moghaddam, M., Martínez Fernández, J., Mattar Bader, C., Morbidelli, R., Musial, J. P., Osenga, E., Palecki, M. A., Pellarin, T., Petropoulos, G. P., Pfeil, I., Powers, J., Robock, A., Rüdiger, C., Rummel, U., Strobel, M., Su, Z., Sullivan, R., Tagesson, T., Varlagin, A., Vreugdenhil, M., Walker, J., Wen, J., Wenger, F., Wigneron, J. P., Woods, M., Yang, K., Zeng, Y., Zhang, X., Zreda, M., Dietrich, S., Gruber, A., van Oevelen, P., Wagner, W., Scipal, K., Drusch, M., and Sabia, R.: The International Soil Moisture Network: serving Earth system science for over a decade, Hydrology and Earth System Sciences, 25, 5749–5804, https://doi.org/10.5194/hess-25-5749-2021, 2021.

Döll, P., Douville, H., Güntner, A., Müller Schmied, H., and Wada, Y.: Modelling Freshwater Resources at the Global Scale: Challenges and Prospects, Surveys in Geophysics, 37, 195–221, https://doi.org/10.1007/s10712-015-9343-1, 2016.

Fick, S. E. and Hijmans, R. J.: WorldClim 2: new 1-km spatial resolution climate surfaces for global land areas, International Journal of Climatology, 37, 4302–4315, https://doi.org/10.1002/joc.5086, 2017.

Freitas, H. R. A., Mendes, C. L., and Ilic, A.: Performance optimization of the MGB hydrological model for multi-core and GPU architectures, Environmental Modelling & Software, 148, 105 271, https://doi.org/10.1016/j.envsoft.2021.105271, 2022.

Freudiger, D., Kohn, I., Seibert, J., Stahl, K., and Weiler, M.: Snow redistribution for the hydrological modeling of alpine catchments, WIREs Water, 4, e1232, https://doi.org/10.1002/wat2.1232, 2017.

Frey, S. and Holzmann, H.: A conceptual, distributed snow redistribution model, Hydrology and Earth System Sciences, 19, 4517–4530, https://doi.org/10.5194/hess-19-4517-2015, 2015.

Ghiggi, G., Humphrey, V., Seneviratne, S. I., and Gudmundsson, L.: GRUN: an observation-based global gridded runoff dataset from 1902 to 2014, Earth System Science Data, 11, 1655–1674, https://doi.org/10.5194/essd-11-1655-2019, 2019.

Haddeland, I., Clark, D. B., Franssen, W., Ludwig, F., Voß, F., Arnell, N. W., Bertrand, N., Best, M., Folwell, S., Gerten, D., Gomes, S., Gosling, S. N., Hagemann, S., Hanasaki, N., Harding, R., Heinke, J., Kabat, P., Koirala, S., Oki, T., Polcher, J., Stacke, T., Viterbo, P., Weedon, G. P., and Yeh, P.: Multimodel Estimate of the Global Terrestrial Water Balance: Setup and First Results, Journal of Hydrometeorology, 12, 869–884, https://doi.org/10.1175/2011JHM1324.1, 2011.

Hanus, S., Schuster, L., Burek, P., Maussion, F., Wada, Y., and Viviroli, D.: Coupling a large-scale glacier and hydrological model (OGGM v1.5.3 and CWatM V1.08) – Towards an improved representation of mountain water resources in global assessments, EGUsphere, pp. 1–31, https://doi.org/10.5194/egusphere-2023-2562, 2024.

Hoch, J. M., Sutanudjaja, E. H., Wanders, N., van Beek, R. L. P. H., and Bierkens, M. F. P.: Hyper-resolution PCR-GLOBWB: opportunities and challenges from refining model spatial resolution to 1 km over the European continent, Hydrology and Earth System Sciences, 27, 1383–1401, https://doi.org/10.5194/hess-27-1383-2023, 2023.

Karger, D. N., Conrad, O., Böhner, J., Kawohl, T., Kreft, H., Soria-Auza, R. W., Zimmermann, N. E., Linder, H. P., and Kessler, M.: Climatologies at high resolution for the earth's land surface areas, Scientific Data, 4, 170 122, https://doi.org/10.1038/sdata.2017.122, 2017.

Knoben, W. J. M., Freer, J. E., and Woods, R. A.: Technical note: Inherent benchmark or not? Comparing Nash–Sutcliffe and Kling–Gupta efficiency scores, Hydrology and Earth System Sciences, 23, 4323–4331, https://doi.org/10.5194/hess-23-4323-2019, 2019.

Kornfeld, R. P., Arnold, B. W., Gross, M. A., Dahya, N. T., Klipstein, W. M., Gath, P. F., and Bettadpur, S.: GRACE-FO: The Gravity Recovery and Climate Experiment Follow-On Mission, Journal of Spacecraft and Rockets, 56, 931–951, https://doi.org/10.2514/1.A34326, 2019.

https://doi.org/10.5194/egusphere-2024-1025
Preprint. Discussion started: 18 April 2024

Kratzert, F., Nearing, G., Addor, N., Erickson, T., Gauch, M., Gilon, O., Gudmundsson, L., Hassidim, A., Klotz, D., Nevo, S., Shalev, G., and Matias, Y.: Caravan - A global community dataset for large-sample hydrology, Scientific Data, 10, 61, https://doi.org/10.1038/s41597-023-01975-w, 2023.

Lange, S., Menz, C., Gleixner, S., Cucchi, M., Weedon, G. P., Amici, A., Bellouin, N., Müller Schmied, H., Hersbach, H., Buontempo, C., and Cagnazzo, C.: WFDE5 over land merged with ERA5 over the ocean (W5E5 v2.0), https://doi.org/10.48364/ISIMIP.342217, type: dataset, 2021.

Lazin, R., Shen, X., Koukoula, M., and Anagnostou, E.: Evaluation of the Hyper-Resolution Model-Derived Water Cycle Components Over the Upper Blue Nile Basin, Journal of Hydrology, 590, 125 231, https://doi.org/10.1016/j.jhydrol.2020.125231, 2020.

Miralles, D. G., De Jeu, R. a. M., Gash, J. H., Holmes, T. R. H., and Dolman, A. J.: Magnitude and variability of land evaporation and its components at the global scale, Hydrology and Earth System Sciences, 15, 967–981, https://doi.org/10.5194/hess-15-967-2011, 2011.

Müller Schmied, H., Eisner, S., Franz, D., Wattenbach, M., Portmann, F. T., Flörke, M., and Döll, P.: Sensitivity of simulated global-scale freshwater fluxes and storages to input data, hydrological model structure, human water use and calibration, Hydrology and Earth System Sciences, 18, 3511–3538, https://doi.org/10.5194/hess-18-3511-2014, 2014.

Nagler, T., Schwaizer, G., Keuris, L., Hetzenecker, M., and Metsämäki, S.: ESA Snow Climate Change Initiative (Snow_cci): Daily global Snow Cover Fraction - snow on ground (SCFG) from MODIS (2000-2019), version 1.0, https://doi.org/10.5285/3B3FD2DAF3D34C1BB4A09EFEAF3B8EA9, 2021.

O'Neill, M. M. F., Tijerina, D. T., Condon, L. E., and Maxwell, R. M.: Assessment of the ParFlow–CLM CONUS 1.0 integrated hydrologic model: evaluation of hyper-resolution water balance components across the contiguous United States, Geoscientific Model Development, 14, 7223–7254, https://doi.org/10.5194/gmd-14-7223-2021, 2021.

Pastorello, G., Trotta, C., Canfora, E., Chu, H., Christianson, D., Cheah, Y.-W., Poindexter, C., Chen, J., Elbashandy, A., Humphrey, M., Isaac, P., Polidori, D., Reichstein, M., Ribeca, A., van Ingen, C., Vuichard, N., Zhang, L., Amiro, B., Ammann, C., Arain, M. A., Ardö, J., Arkebauer, T., Arndt, S. K., Arriga, N., Aubinet, M., Aurela, M., Baldocchi, D., Barr, A., Beamesderfer, E., Marchesini, L. B., Bergeron, O., Beringer, J., Bernhofer, C., Berveiller, D., Billesbach, D., Black, T. A., Blanken, P. D., Bohrer, G., Boike, J., Bolstad, P. V., Bonal, D., Bonnefond, J.-M., Bowling, D. R., Bracho, R., Brodeur, J., Brümmer, C., Buchmann, N., Burban, B., Burns, S. P., Buysse, P., Cale, P., Cavagna, M., Cellier, P., Chen, S., Chini, I., Christensen, T. R., Cleverly, J., Collalti, A., Consalvo, C., Cook, B. D., Cook, D., Coursolle, C., Cremonese, E., Curtis, P. S., D'Andrea, E., da Rocha, H., Dai, X., Davis, K. J., Cinti, B. D., Grandcourt, A. d., Ligne, A. D., De Oliveira, R. C., Delpierre, N., Desai, A. R., Di Bella, C. M., Tommasi, P. d., Dolman, H., Domingo, F., Dong, G., Dore, S., Duce, P., Dufrêne, E., Dunn, A., Dušek, J., Eamus, D., Eichelmann, U., ElKhidir, H. A. M., Eugster, W., Ewenz, C. M., Ewers, B., Famulari, D., Fares, S., Feigenwinter, I., Feitz, A., Fensholt, R., Filippa, G., Fischer, M., Frank, J., Galvagno, M., Gharun, M., Gianelle, D., Gielen, B., Gioli, B., Gitelson, A., Goded, I., Goeckede, M., Goldstein, A. H., Gough, C. M., Goulden, M. L., Graf, A., Griebel, A., Gruening, C., Grünwald, T., Hammerle, A., Han, S., Han, X., Hansen, B. U., Hanson, C., Hatakka, J., He, Y., Hehn, M., Heinesch, B., Hinko-Najera, N., Hörtnagl, L., Hutley, L., Ibrom, A., Ikawa, H., Jackowicz-Korczynski, M., Janouš, D., Jans, W., Jassal, R., Jiang, S., Kato, T., Khomik, M., Klatt, J., Knohl, A., Knox, S., Kobayashi, H., Koerber, G., Kolle, O., Kosugi, Y., Kotani, A., Kowalski, A., Kruijt, B., Kurbatova, J., Kutsch, W. L., Kwon, H., Launiainen, S., Laurila, T., Law, B., Leuning, R., Li, Y., Liddell, M., Limousin, J.-M., Lion, M., Liska, A. J., Lohila, A., López-Ballesteros, A., López-Blanco, E., Loubet, B., Loustau, D., Lucas-Moffat, A., Lüers, J., Ma, S., Macfarlane, C., Magliulo, V., Maier, R., Mammarella, I., Manca, G., Marcolla, B., Margolis, H. A., Marras, S., Massman, W., Mastepanov, M., Matamala, R., Matthes, J. H., Mazzenga, F., McCaughey, H., McHugh, I., McMillan, A. M. S., Merbold, L., Meyer, W., Meyers, T., Miller, S. D., Minerbi, S., Moderow, U., Monson, R. K., Montagnani, L., Moore, C. E., Moors, E., Moreaux, V., Moureaux, C., Munger, J. W., Nakai, T., Neirynck,

https://doi.org/10.5194/egusphere-2024-1025
Preprint. Discussion started: 18 April 2024

J., Nesic, Z., Nicolini, G., Noormets, A., Northwood, M., Nosetto, M., Nouvellon, Y., Novick, K., Oechel, W., Olesen, J. E., Ourcival, J.-M., Papuga, S. A., Parmentier, F.-J., Paul-Limoges, E., Pavelka, M., Peichl, M., Pendall, E., Phillips, R. P., Pilegaard, K., Pirk, N., Posse, G., Powell, T., Prasse, H., Prober, S. M., Rambal, S., Rannik, , Raz-Yaseef, N., Rebmann, C., Reed, D., Dios, V. R. d., Restrepo-Coupe, N., Reverter, B. R., Roland, M., Sabbatini, S., Sachs, T., Saleska, S. R., Sánchez-Cañete, E. P., Sanchez-Mejia, Z. M., Schmid, H. P., Schmidt, M., Schneider, K., Schrader, F., Schroder, I., Scott, R. L., Sedlák, P., Serrano-Ortíz, P., Shao, C., Shi, P., Shironya, I., Siebicke, L., Šigut, L., Silberstein, R., Sirca, C., Spano, D., Steinbrecher, R., Stevens, R. M., Sturtevant, C., Suyker, A., Tagesson, T., Takanashi, S., Tang, Y., Tapper, N., Thom, J., Tomassucci, M., Tuovinen, J.-P., Urbanski, S., Valentini, R., van der Molen, M., van Gorsel, E., van Huissteden, K., Varlagin, A., Verfaillie, J., Vesala, T., Vincke, C., Vitale, D., Vygodskaya, N., Walker, J. P., Walter-Shea, E., Wang, H., Weber, R., Westermann, S., Wille, C., Wofsy, S., Wohlfahrt, G., Wolf, S., Woodgate, W., Li, Y., Zampedri, R., Zhang, J., Zhou, G., Zona, D., Agarwal, D., Biraud, S., Torn, M., and Papale, D.: The FLUXNET2015 dataset and the ONEFlux processing pipeline for eddy covariance data, Scientific Data, 7, 225, https://doi.org/10.1038/s41597-020-0534-3, 2020.

Schär, C., Fuhrer, O., Arteaga, A., Ban, N., Charpilloz, C., Girolamo, S. D., Hentgen, L., Hoefler, T., Lapillonne, X., Leutwyler, D., Osterried, K., Panosetti, D., Rüdisühli, S., Schlemmer, L., Schulthess, T. C., Sprenger, M., Ubbiali, S., and Wernli, H.: Kilometer-Scale Climate Models: Prospects and Challenges, Bulletin of the American Meteorological Society, 101, E567–E587, https://doi.org/10.1175/BAMS-D-18-0167.1, 2020.

Singh, R. S., Reager, J. T., Miller, N. L., and Famiglietti, J. S.: Toward hyper-resolution land-surface modeling: The effects of fine-scale topography and soil texture on CLM 4.0 simulations over the S outhwestern U.S., Water Resources Research, 51, 2648–2667, https://doi.org/10.1002/2014WR015686, 2015.

Sutanudjaja, E. H., van Beek, L. P. H., de Jong, S. M., van Geer, F. C., and Bierkens, M. F. P.: Large-scale groundwater modeling using global datasets: a test case for the Rhine-Meuse basin, Hydrology and Earth System Sciences, 15, 2913–2935, https://doi.org/10.5194/hess-15-2913-2011, 2011.

Sutanudjaja, E. H., van Beek, R., Wanders, N., Wada, Y., Bosmans, J. H. C., Drost, N., van der Ent, R. J., de Graaf, I. E. M., Hoch, J. M., de Jong, K., Karssenberg, D., López López, P., Peßenteiner, S., Schmitz, O., Straatsma, M. W., Vannametee, E., Wisser, D., and Bierkens, M. F. P.: PCR-GLOBWB 2: a 5 arcmin global hydrological and water resources model, Geoscientific Model Development, 11, 2429–2453, https://doi.org/10.5194/gmd-11-2429-2018, 2018.

Towner, J., Cloke, H. L., Zsoter, E., Flamig, Z., Hoch, J. M., Bazo, J., Coughlan de Perez, E., and Stephens, E. M.: Assessing the performance of global hydrological models for capturing peak river flows in the Amazon basin, Hydrology and Earth System Sciences, 23, 3057–3080, https://doi.org/10.5194/hess-23-3057-2019, 2019.

van Beek, L. P. H.: Forcing PCR-GLOWB with CRU data, Tech. rep., Department of Physical Geography, Utrecht University,, https://vanbeek.geo.uu.nl/suppinfo/vanbeek2008.pdf, 2008.

van Beek, L. P. H. and Bierkens, M. F. P.: The Global Hydrological Model PCR-GLOBWB: Conceptualization, and Verification, Tech. rep., Department of Physical Geography, Utrecht University,, http://vanbeek.geo.uu.nl/suppinfo/vanbeekbierkens2009.pdf, 2008.

Van Beek, L. P. H., Wada, Y., and Bierkens, M. F. P.: Global monthly water stress: 1. Water balance and water availability, Water Resources Research, 47, 2010WR009 791, https://doi.org/10.1029/2010WR009791, 2011.

Vergopolan, N., Chaney, N. W., Pan, M., Sheffield, J., Beck, H. E., Ferguson, C. R., Torres-Rojas, L., Sadri, S., and Wood, E. F.: SMAP-HydroBlocks, a 30-m satellite-based soil moisture dataset for the conterminous US, Scientific Data, 8, 264, https://doi.org/10.1038/s41597-021-01050-2, 2021.

https://doi.org/10.5194/egusphere-2024-1025
Preprint. Discussion started: 18 April 2024

Vremec, M. and Collenteur, R.: PyEt - a Python package to estimate potential and reference evapotranspiration, Tech. Rep. EGU21-15008, Copernicus Meetings, https://doi.org/10.5194/egusphere-egu21-15008, 2021.

Vörösmarty, C. J., Hoekstra, A. Y., Bunn, S. E., Conway, D., and Gupta, J.: Fresh water goes global, Science, 349, 478–479, https://doi.org/10.1126/science.aac6009, 2015.

Wada, Y., Bierkens, M. F. P., de Roo, A., Dirmeyer, P. A., Famiglietti, J. S., Hanasaki, N., Konar, M., Liu, J., Müller Schmied, H., Oki, T., Pokhrel, Y., Sivapalan, M., Troy, T. J., van Dijk, A. I. J. M., van Emmerik, T., Van Huijgevoort, M. H. J., Van Lanen, H. A. J., Vörösmarty, C. J., Wanders, N., and Wheater, H.: Human–water interface in hydrological modelling: current status and future directions, Hydrology and Earth System Sciences, 21, 4169–4193, https://doi.org/10.5194/hess-21-4169-2017, 2017.

Wiersma, P., Aerts, J., Zekollari, H., Hrachowitz, M., Drost, N., Huss, M., Sutanudjaja, E. H., and Hut, R.: Coupling a global glacier model to a global hydrological model prevents underestimation of glacier runoff, Hydrology and Earth System Sciences, 26, 5971–5986, https://doi.org/10.5194/hess-26-5971-2022, 2022.

Wilby, R. L., Hay, L. E., Gutowski, W. J., Arritt, R. W., Takle, E. S., Pan, Z., Leavesley, G. H., and Clark, M. P.: Hydrological responses to dynamically and statistically downscaled climate model output, Geophysical Research Letters, 27, 1199–1202, https://doi.org/10.1029/1999GL006078, 2000.

Wood, E. F., Roundy, J. K., Troy, T. J., Van Beek, L. P. H., Bierkens, M. F. P., Blyth, E., De Roo, A., Döll, P., Ek, M., Famiglietti, J., Gochis, D., Van De Giesen, N., Houser, P., Jaffé, P. R., Kollet, S., Lehner, B., Lettenmaier, D. P., Peters-Lidard, C., Sivapalan, M., Sheffield, J., Wade, A., and Whitehead, P.: Hyperresolution global land surface modeling: Meeting a grand challenge for monitoring Earth's terrestrial water, Water Resources Research, 47, 2010WR010 090, https://doi.org/10.1029/2010WR010090, 2011.

Yang, C., Tijerina-Kreuzer, D., Tran, H., Condon, L., and Maxwell, R.: A high-resolution, 3D groundwater-surface water simulation of the contiguous US: Advances in the integrated ParFlow CONUS 2.0 modeling platform, https://eartharxiv.org/repository/view/5670/, 2023.